Environ. Sci. Technol. **1997**, *31*, 2854−2858

Iron Nodules Scavenging Uranium from Groundwater

TSUTOMU SATO,*,† TAKASHI MURAKAMI,‡ NOBUYUKI YANASE,† HIROSHI ISOBE,† TIMOTHY E. PAYNE,§ AND PETER L. AIREY§

Department of Environmental Safety Research, Japan Atomic Energy Research Institute, Tokai, Ibaraki 319-11, Japan, Mineralogical Institute, University of Tokyo, Bunkyo-ku, Tokyo 113, Japan, and Australian Nuclear Science and Technology Organisation, PMB 1, Menai, New South Wales 2234, Australia

The scavenging of uranium from groundwater downgradient of the uranium ore deposit at Koongarra, Australia, has been investigated to provide information about the long-term transport of radionuclides. Rock samples collected from diamond-drill cores were examined mainly using scanning and transmission electron microscopy. Here we focus on the U associated with iron oxides and report on (i) the extent to which U has accumulated in the various types of iron oxides (fissure fillings, clay coatings, and nodules) and (ii) the chemical form of U associated with iron-nodules. The iron nodules have a remarkably large capacity for uranium uptake. The uranium enrichment in the nodules reaches approximately 8 wt %, and their uranium contents are greater than those in the other iron forms, such as fissure fillings and clay coatings. The ability of the iron nodules to enrich uranium (to levels 10^6 times higher than the groundwater) is greater than those of any other natural materials in the system. Although the initial step in uranium uptake appears to be adsorption, the uranium in the nodules has been fixed by precipitation of copper uranyl phosphate microcrystals. This precipitation process leads to the long-term retardation of uranium in the system. This result strongly suggests that an understanding of post-adsorption processes is necessary for predicting radionuclide retardation over long time scales.

Introduction

Under oxidizing conditions, uranium (U) is much more mobile in the environment than it is in reducing conditions. However, the mobility of dissolved U in both seawater and groundwater can be retarded by precipitation of U-bearing materials and, particularly at low U concentrations, by adsorption to various geomaterials. For the modeling of U transport, it is important to determine the relative importance of these two mechanisms. Numerous studies have reported that U is generally associated with iron oxides, hydroxides, and oxyhydroxides (hereafter grouped generically as iron oxides) in the subsurface environment (*1*−*13*). An understanding of the interaction between U and iron oxides is therefore important for assessing the retardation capacity of geological systems into which U may be disposed, such as U mine waste dumps and radioactive waste repositories. Although most of the previous studies have emphasized the importance of Fe phases in adsorption of U, less attention has been paid to their capacity for U uptake and to the post-adsorption behavior of U in iron oxides.

The Koongarra U ore deposit in Australia, from which U has been mobilized by water−rock interactions in the past 1−3 million years (*14*, *15*), is a suitable site to follow the fate of U in circumstances where groundwater U concentrations are relatively high. At Koongarra, both re-precipitation of mobilized U as secondary minerals and association of U with iron oxides are observed (*14*). Here we focus on the U associated with iron oxides and report on (i) the extent to which U has accumulated in the various types of iron oxides (fissure fillings, clay coatings, and nodules) and (ii) the chemical form of U associated with Fe nodules.

Sampling Sites and Experimental Section

The Koongarra uranium deposit lies about 225 km east of Darwin in the Northern Territory of Australia. The primary ore body was formed at ca. 1.6 billion years ago by the precipitation of uraninite in close proximity to a graphite layer in the quartz chlorite schist (*14*). As a result of the leaching of the primary ore zone and transport of U by groundwater, a tongue-like "dispersion fan", (a region of ore-grade material) has formed in the most recent 1−3 million years (Figure 1). Within the primary ore zone, uranyl silicates (sklodowskite) have been produced by in-situ oxidation and alteration. The secondary mineralization in the zone above the primary ore is characterized by uranyl phosphates (saléeite), which are frequently found as aggregates observable with the naked eye. The weathering of uraninite to secondary U-bearing minerals has occurred concurrently with the alteration of chlorite [$(Mg,Fe,Al)_6(Al,Si)_4O_{10}(OH)_8$] to clays and iron oxides. Downstream of the primary ore zone, the U is associated with weathering products, especially the iron oxides in the dispersed ore zone (*4*, *10*−*13*).

The rock samples used in this study were collected from diamond-drill cores (DDH) drilled at an angle of about 50° from the horizontal to facilitate core recovery and intersect strata. The samples were collected at intervals of 3 m in depth (from 3 to 30 m) and analyzed mineralogically and radiochemically.

Polished thin sections of the samples were examined by optical microscopy, followed by scanning electron microscopy (SEM) with energy dispersive X-ray analysis (EDX), analytical electron microscopy (AEM), and micro-infrared and visible (micro-IR and VIS) spectroscopies to identify the mineral species and to examine the textures of the samples. For quantitative element analysis, the EDX spectra were collected for 200 s at an operating voltage of 20 kV and a beam current of 0.1 nA. The analyses were corrected for matrix effects (atomic number, absorption, and fluorescence) using a standard routine. Powdered bulk samples were examined by γ-spectrometry to measure the uranium contents (see ref *16* for further details).

Results and Discussion

Previous mineralogical studies at Koongarra have shown that goethite (α-FeOOH), hematite (α-Fe_2O_3), and ferrihydrite ($Fe_5HO_8{\cdot}4H_2O$) are the major Fe minerals in the weathered zone (*11*−*13*). Sub-micrometer-sized grains of iron oxides are found at domain boundaries, and larger accumulations are located within grain boundaries, fissures, and the voids produced during mineral dissolution. The accumulated Fe minerals occur in particular morphological features such as fissure fillings, dispersed clay coatings, and nodules.

* Corresponding author telephone: +81-29-282-6180; fax: +81-29-282-5958; e-mail: sato@sparclt.tokai.jaeri.go.jp.
† Japan Atomic Energy Research Institute.
‡ University of Tokyo.
§ Australian Nuclear Science and Technology Organisation.

S0013-936X(97)00058-8 CCC: $14.00

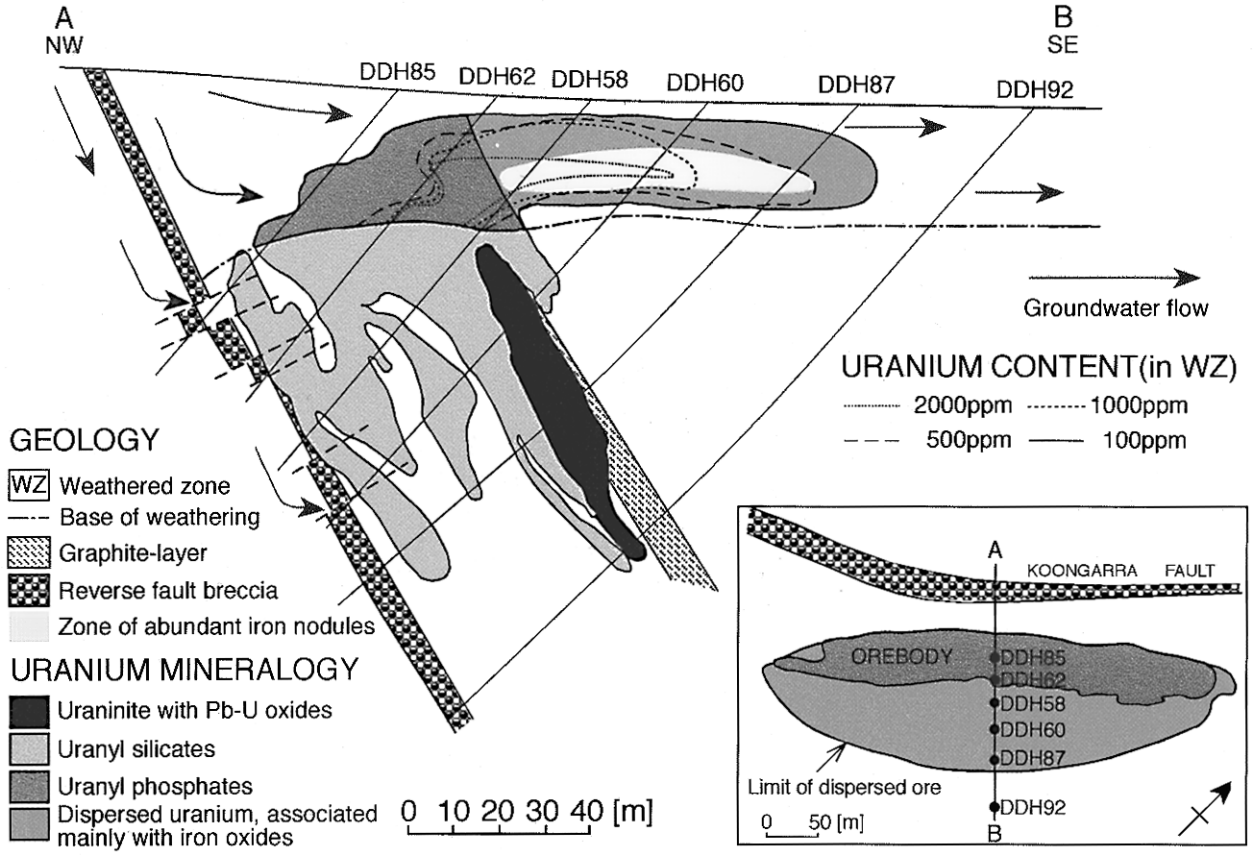

FIGURE 1. Cross-section of the Koongarra ore body showing the geology, distribution of uranium minerals, zone of abundant iron nodules, and contours of uranium contents in weathered bulk samples. The insert in the bottom right-hand corner shows locations of the holes from which the samples were collected (plan view).

The iron oxides observed in the clay coatings and fissures are black or dark brown (Figure 2), whereas iron oxides in the nodules have a yellow, orange, or reddish brown color. The nodules are dark brown only when residual silicate minerals from weathering are still present. The Fe nodules, when observed under the petrographic microscope, have very irregular shapes, in many cases having a complex alveolar structure, and have an average size of several hundred micrometers across. The centers of the nodules are void in cases where there is no mineral inclusion. However, when inclusions are present, the Fe nodules are well developed and there is no void in the center (Figure 2C). Most of the Fe nodules are surrounded by kaolinite [$Al_2Si_2O_5(OH)_4$], a weathering product of the host rock. The U distribution is controlled by the mineralogy; the Fe nodules contain high concentrations of U, whereas the kaolinite has virtually no U (Figure 2B).

Quantitative analysis of the iron oxides by SEM/EDX shows that there is a considerable variation in the amount of U associated with each form of iron oxide. The nodules usually have high U contents (up to approximately 8 wt % as UO_3) as compared to the other Fe forms (Table 1). Iron oxides are ubiquitous in the dispersion fan and also the surrounding weathered rocks. However, Fe nodules are restricted to the center of the dispersion fan (Figure 1), which is also an area of high U content. The U in the groundwater is only 10−100 ppb in the vicinity of secondary ore deposit (*13, 17*) and is undersaturated with respect to the U minerals that are present (*18*). The high U content of the solid phase in the center of dispersion fan is therefore largely attributable to the U-rich Fe nodules. This suggests that the Fe nodules play a key role in the scavenging and retention of U downgradient of the secondary ore zone, where no uranyl silicates and phosphates have been observed.

Within the Fe nodules, the U content is variable and is related to the color of Fe materials. It is greatest in the yellow zones and then decreasingly found in the orange, brown, and black zones (Table 1 and the X-ray map in Figure 2B). Micro-IR and VIS spectroscopies showed that the yellow material is goethite and that the black zone contains an amorphous Fe material (probably ferrihydrite). The brown and orange zones are probably intermediate phases and include a small amount of hematite. The order of decreasing U content therefore corresponds to the order of decreasing crystallinity of the iron oxides. Generally, amorphous iron oxides, precursor materials of crystalline iron oxides, have a higher adsorption capacity than the crystalline phases due to their larger specific surface areas as shown by the enrichment factors for U adsorption under the same experimental conditions (e.g., amorphous iron oxides; $1.1-2.7 \times 10^6$, natural goethite; 4×10^3) (*4*). However, at Koongarra, the goethite in the nodules has a higher U content than the amorphous iron oxides in the coatings and fissures (Table 1). This result suggests that the U enrichment in the goethite cannot be explained by adsorption alone.

The SEM/EDS examination showed that the U-rich Fe nodules contain aluminum, silicon, phosphorus (P), copper (Cu), and occasionally magnesium, titanium, vanadium, chromium, manganese, and nickel. Of these elements, the U content of the nodules is positively correlated only with P and Cu (Figure 3), suggesting the formation of a phase containing these elements.

In common with uranyl, phosphate and Cu ions are strongly adsorbed on iron oxides (*19−27*). The uptake of phosphate generally induces an increase in the cation exchange capacity by the creation of additional negative charge. However, Cu ions compete against uranyl ions in adsorption; therefore, the presence of Cu may interfere with

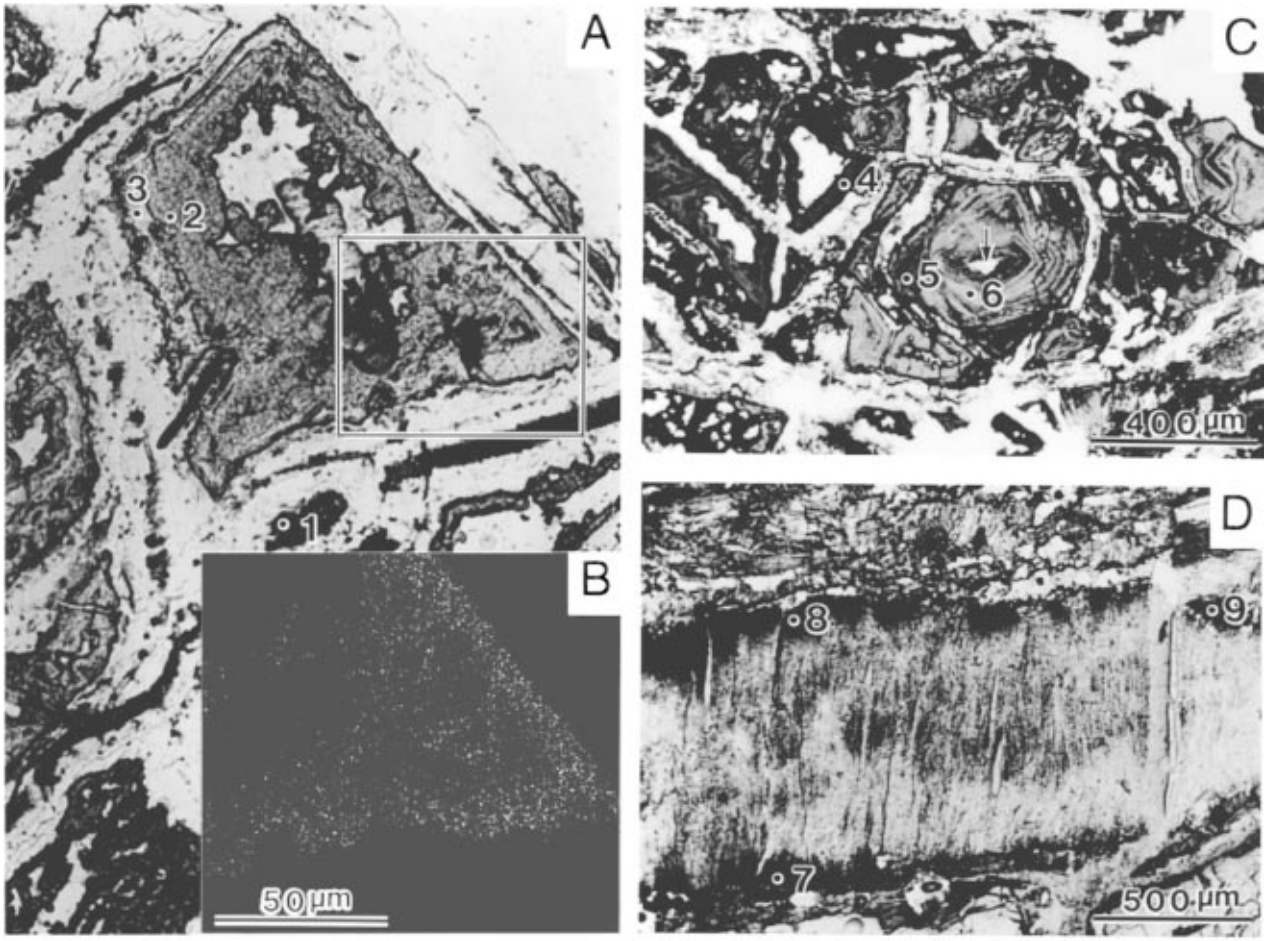

FIGURE 2. Micrographs of iron nodules and Fe material coatings. Optical micrographs of thin sections were taken under transmitted light with no polarizer. (A) Iron nodules of DDH58 18.2 m are characterized by a zonal structure having a yellow, orange, and brown color. In the center of the large nodules is a natural void, which has been filled with epoxy resin during thin section preparation. (B) X-ray map of uranium, obtained by wavelength dispersive spectrometry, from the enclosed area with a rectangle in panel A. The rim of the nodule is yellow, and regions of higher uranium content correspond with a higher density of dots. (C) Iron nodules from DDH60 15.2 m with orange and reddish brown colors. The largest nodule has a garnet inclusion (arrowed). (D) Kaolinite (transparent) from DDH58 12.1 m coated with amorphous iron materials (opaque). The transparent minerals surrounding iron nodules in panels A and C are also kaolinite. The numbers in each figure are measuring points of uranium contents corresponding to those in Table 1.

TABLE 1. Comparison of Uranium Contents among Various Iron Forms[a]

iron forms	nodules							coatings			fissures	
DDH no.	58			60			87	58			60	
depth (m)	18.2			15.2			15.2	12.1			15.2	12.1
U in bulk (ppm)[b]	4543			2172			773	1688			2172	1173
measuring point[c]	1	2	3	4	5	6	NS	7	8	9	NS	NS
UO_3 (wt%)[d]	1.9	4.3	7.7	2.4	2.9	4.6	1.6	0.7	0.5	0.6	0.5	ND
color	Br	O	Y	RBr	RBr	O	RBr	Bk	Bk	Bk	BK	Bk

[a] Abbreviations: DDH no., diamond-drill hole number; NS, position not shown in Figure 2; ND, not detected; Br, brown; O, orange; Y, yellow; Rbr, reddish brown; Bk, black. [b] Uranium contents of bulk samples were measured by γ-spectrometry. [c] Measuring points are shown by corresponding numbers in Figure 2. [d] Uranium contents were measured by SEM/EDX. These values are weight percentages of UO_3.

U adsorption on iron oxides. The positive correlation of U content with both Cu and P in the Fe nodules suggests that the U retention may be due to precipitation rather than adsorption, possibly as copper uranyl phosphate, i.e., torbernite or metatorbernite $[Cu(UO_2)_2(PO_4)_2 \cdot 8-12H_2O]$.

In order to observe the U-bearing phases, Fe nodules in sample DDH60 15.2 m (same sample shown in Figure 2C) were examined further by AEM, which has a superior spatial resolution to SEM/EDX. Although phases containing only U, P, and Cu were not detected, scattered domains (about 20 nm) with high U, P and Cu were observed in the matrices of the large iron oxide particles. This observation strongly indicates that U associated with P, and Cu was not only adsorbed on the surfaces of the individual Fe particles but also incorporated as microcrystalline torbernite or metatorbernite scattered in the matrices of the iron oxides.

Saléeite $[Mg(UO_2)_2(PO_4)_2 \cdot 8-10H_2O]$ is present at the upstream edge of the secondary ore deposit (Figure 1) as visible crystals that are not associated with iron minerals. In this region close to the primary ore body, U concentrations in the groundwater are relatively high, and the Mg concentrations greatly exceed those of other cations due to the weathering of Mg-rich chlorite. Phosphate concentrations are also relatively high close to the primary ore zone (*13*).

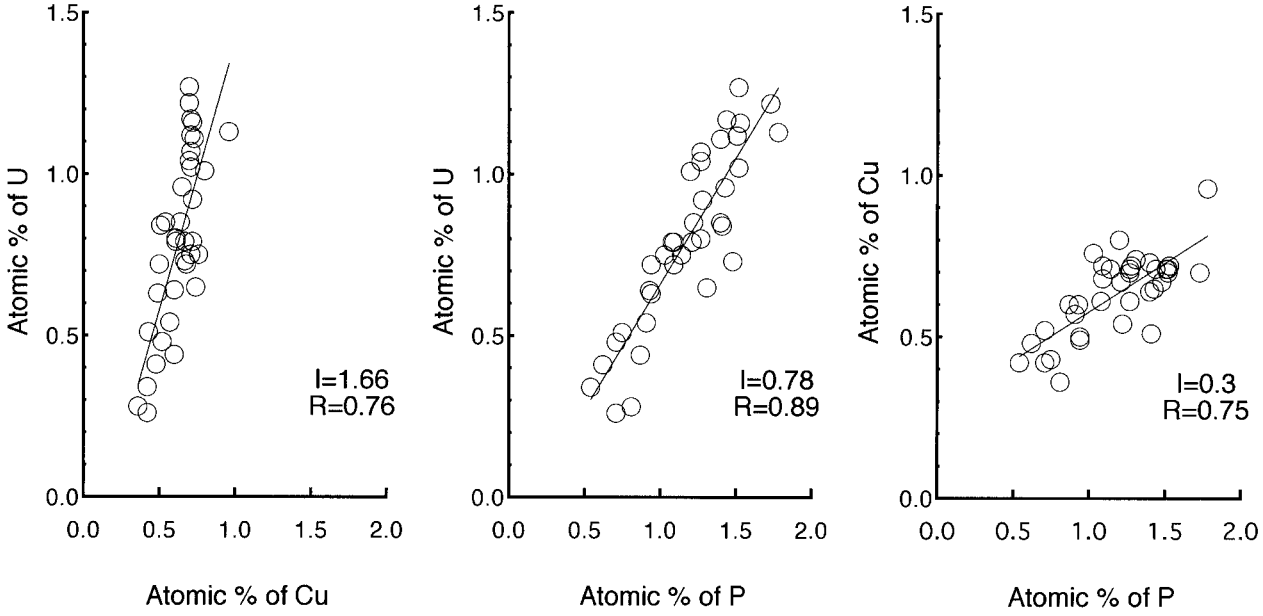

FIGURE 3. Relationships between atomic percentage of uranium (U) and copper (Cu), U and phosphorus (P), and Cu and P in the iron nodules of DDH58 18.2 m (shown in Figure 2A). The atomic percentages of each element were measured by SEM/EDX. The values of *I* and *R* in each figure are the inclination and the coefficient of correlation of fitting line, respectively. Each of the correlations shown in the figure is significant at the $p < 0.001$ level. There were no significant correlations observed between any other elements contained in the Fe nodules.

Consequently, the saléeite appears to have formed by direct precipitation, which is a different mechanism to that proposed for the formation of torbernite or metatorbernite within the Fe nodules. Iron oxides strongly bind Cu, P, and U in the circumneutral pH range (*19*−*27*), whereas adsorption of Mg is weaker and occurs in the pH range above 7 (*28*). Consequently, when the contacting groundwater contains Cu, the microcrystalline phase forming within the Fe nodules is a copper uranyl phosphate mineral rather than a Mg-containing phase such as saléeite. Although the contacting groundwater is currently undersaturated with respect to torbernite or metatorbernite, several experimental and theoretical studies have shown that the surface of various oxides may induce precipitation when the bulk solution is still undersaturated with respect to the precipitated phase (*29*, *30*). The precipitation of torbernite or metatorbernite in the Fe nodules would be consistent with these results.

Textural relationships in the samples suggest that the crystalline Fe minerals in the nodules result from conversion of the amorphous materials. As mentioned above, most of the Fe nodules we observed were surrounded by kaolinite (Figure 2). The peripheral kaolinite appears to play an important role in producing the physicochemical conditions conducive to this conversion. Further work is required to elucidate the mechanism of the development of Fe nodules and to study the role of the peripheral kaolinite.

In this paper, we have shown that the Fe nodules are important in immobilizing U in the Koongarra dispersion fan. In previous studies of the association between U and iron oxides, the reported levels of U scavenged by iron oxides are commonly in the ppm range (*3*, *31*) but occasionally approach 0.1−1% (*5*, *8*) under environmental conditions. The Fe nodules at Koongarra, with approximately 8% of U, therefore have a remarkably high scavenging capacity, even allowing for the large amount of uranium available by weathering of the primary U ore. The ability of the Fe nodules to enrich U (10^6 times higher than the groundwater) is also very high. The enrichment factor of the Fe nodules exceeds those of other natural scavengers such as microorganisms (10^3 times) (*32*), marine ferromanganese nodules (10^3 times) (*3*, *31*), and suspended particulates in river (10^3−10^5 times) (*33*).

The initial interaction of U with iron oxides is probably by adsorption, but there is a subsequent mineralization process leading to the formation of U-bearing phases with very high U contents in the Fe nodules. This post-adsorption process occurs during aging and conversion of iron oxides. This process is an important immobilization mechanism leading to the long-term retardation of U in the system. In the absence of these processes occurring in the weathered zone of Koongarra, the U would have presumably been dispersed much more widely. Many previous studies have focused on the types and amounts of adsorbing materials for radionuclide immobilization in geological systems. This study illustrates that, even if all possible sorbing phases are considered, long-term predictions as to the fate of U are incomplete without an understanding of post-adsorption processes related to evolution of the associated materials over the long term.

Acknowledgments

We thank Dr. A. A. Snelling for the collection of the samples and S. Leung and M. G. Blackford of Australian Nuclear Science and Technology Organisation for technical support of the part of AEM and SEM/EDX studies.

Literature Cited

(1) Koons, R. D.; Helmke, P. A.; Jackson, M. L. *Soil Sci. Soc. Am. J.* **1980**, *44*, 155−159.
(2) Gueniot, B.; Guillet, B.; Souchier, B. *C. R. C. Acad. Sci. Ser. 2* **1982**, *251*, 31−36.
(3) Kunzendorf, H.; Glasby, G. P.; Plüger, W. L.; Friedrich, G. H. *Uranium* **1982**, *1*, 19−36.
(4) Gray, D. J. Ph.D. Dissertation, University of Sydney, 1986.
(5) Guthrie, V. A.; Kleeman, J. D. *Chem. Geol.* **1986**, *54*, 113−126.
(6) Smellie, J. A. T.; MacKenzie, A. B.; Scott, R. D. *Chem. Geol.* **1986**, *55*, 233−254.
(7) Zielinski, R. A.; Bush, C. A.; Spengler, R. W.; Szabo, B. J. *Uranium* **1986**, *2*, 361−386.
(8) Ilani, S.; Kronfeld, J.; Pinchasov, A. *Uranium* **1987**, *4*, 159−174.
(9) Milton, G. M.; Brown, R. M. *Can. J. Earth Sci.* **1987**, *24*, 1321−1328.
(10) Yanase, N.; Nightingale, T.; Payne, T. E.; Duerden, P. *Radiochim. Acta* **1991**, *52/53*, 387−393.
(11) Edis, R.; et al. *Alligator Rivers Analogue Project Final Report*, Vol. 8; ISBN 0-642-59934-3; Australian Nuclear Science and Technology Organisation: Sydney, 1992.

(12) Murakami, T.; et al. *Alligator Rivers Analogue Project Final Report*, Vol. 9 ISBN 0-642-59935-1; Australian Nuclear Science and Technology Organisation: Sydney, 1992.
(13) Payne, T. E.; et al. *Alligator Rivers Analogue Project Final Report*, Vol. 7; ISBN 0-642-59933-5, Australian Nuclear Science and Technology Organisation: Sydney, 1992.
(14) Snelling, A. A. *Alligator Rivers Analogue Project Final Report*, Vol. 2; ISBN 0-642-59928-9; Australian Nuclear Science and Technology Organisation: Sydney, 1992.
(15) Airey, P. L. *Chem. Geol.* **1986**, *55*, 255−268.
(16) Yanase, N.; Sekine, K. *Mat. Res. Soc. Symp. Proc.* **1995**, *353*, 1235−1242.
(17) Yanase, N.; Payne, T. E.; Sekine, K. *Geochem. J.* **1995**, *29*, 1−29.
(18) Sverjensky, D. A. *Alligator Rivers Analogue Project Final Report*, Vol. 12; ISBN 0-642-59938-6, Australian Nuclear Science and Technology Organisation: Sydney, 1992.
(19) Hingston, D. D.; Atkinson, R. J.; Posner, A. M.; Quirk, J. P. *Trans. Int. Congr. Soil Sci., 9th* **1968**, *I*, 669−678.
(20) Atkinson, R. J.; Posner, A. M.; Quirk, J. P. J. *Inorg. Nucl. Chem.* **1972**, *34*, 2201−2209.
(21) Russell, J. D.; Parfitt, R. L.; Fraser, A. R.; Farmer, V. C. *Nature* **1974**, *248*, 220−221.
(22) MacKenzie, R. M. *Aust. J. Soil Res.* **1980**, *18*, 61−73.
(23) Sigg, L.; Stumm, W. *Colloids Surf.* **1981**, *2*, 101−117.
(24) Padmanabham, M. *Aust. J. Soil Res.* **1983**, *21*, 309−320.
(25) Padmanabham, M. *Aust. J. Soil Res.* **1983**, *21*, 515−525.
(26) Dzombak, D. A.; Morel, F. M. M. *Surface complexation modeling*; John Wiley & Sons: New York 1990.
(27) Payne, T. E.; Davis, J. A.; Waite, T. D. *Radiochim. Acta* **1996**, *74*, 239−243.
(28) Balistrieri, L. S.; Murray, J. W. *Am. J. Sci.* **1981,** *281*, 788−806.
(29) James, R. O.; Healy, T. W. *J. Colloid Interface Sci.* **1972**, *40*, 42−52.
(30) James, R. O.; Healy, T. W. *J. Colloid Interface Sci.* **1972**, *40*, 65−81.
(31) Huh, C. A.; Ku, T. L. *Geochim. Cosmochim. Acta* **1984**, *48*, 951−963.
(32) Strandberg, G. W.; Shumate, S. T.; Parrott, J. R. J. *Appl. Environ. Microbiol.* **1981**, *41*, 237−245.
(33) Mann, H.; Fyfe, W. S. *Uranium* **1987**, *4*, 175−192.

Received for review January 27, 1997. Revised manuscript received May 29, 1997. Accepted June 18, 1997.[⊗]

ES970058M

[⊗] Abstract published in *Advance ACS Abstracts,* August 1, 1997.